Research Paper

https://doi.org/10.7733/jnfcwt.2024.032

Thermodynamics of Se(IV) Sorption Onto Ca-type Bentonil-WRK Montmorillonite

Seonggyu Choi[1,*], Ja-Young Goo[1], Jeonghwan Hwang[1], Yongheum Jo[2], Jae-Kwang Lee[1], and Jang-Soon Kwon[1]

[1]*Korea Atomic Energy Research Institute, 111, Daedeok-daero 989beon-gil, Yuseong-gu, Daejeon 34057, Republic of Korea*

[2]*Hanyang University, 222, Wangsimni-ro, Seongdong-gu, Seoul 04763, Republic of Korea*

(Received June 4, 2024 / Revised July 3, 2024 / Approved August 12, 2024)

Se sorption onto Ca-type montmorillonite purified from Bentonil-WRK—a new research bentonite introduced by Korea Atomic Energy Research Institute—was examined under ambient conditions (pH 4–9, pe 7–9, I = 0.01 M $CaCl_2$, and T = 25°C). Se(IV) was identified as the oxidation state responsible for weak sorption (Kd < 22 $L \cdot kg^{-1}$) by forming surface complexes with edge functional groups of the montmorillonite. Thermodynamic modeling, considering reaction mechanisms of outer-sphere complexation ($\equiv AlOH_2^+ + HSeO_3^- \rightleftharpoons \equiv AlOH_3SeO_3$, log K = 0.50 ± 0.21), inner-sphere complexation ($2\equiv AlOH + H_2SeO_3(aq) \rightleftharpoons (\equiv Al)_2SeO_3 + 2H_2O(l)$, log K = 7.89 ± 0.51), and Ca^{2+}-involved ternary complexation ($\equiv AlOH + Ca^{2+} + SeO_3^{2-} \rightleftharpoons \equiv AlOHCaSeO_3$, log K = 7.69 ± 0.28) between selenite and aluminol sites of montmorillonite, acceptably reproduced the batch sorption data. Outer- and inner-sphere complexes are predominant Se(IV) forms sorbed in acidic (pH ≈ 4) and near-acidic (pH ≈ 6) regions, respectively, whereas ternary complexation accounts for Se(IV) sorption at neutral pHs under the ambient conditions. The experimental and modeling data generally extend a material-specific sorption database of Bentonil-WRK, which is essential for assessing its radionuclide retention performance as a buffer candidate of deep geological disposal system for high-level radioactive waste.

Keywords: Bentonite, Montmorillonite, Bentonil-WRK, Selenium, Thermodynamic sorption modeling, Surface complexation

*Corresponding Author.
Seonggyu Choi, Korea Atomic Energy Research Institute, E-mail: schoi21@kaeri.re.kr, Tel: +82-42-866-6459

ORCID

Seonggyu Choi	http://orcid.org/0000-0002-5784-5034	Ja-Young Goo	http://orcid.org/0000-0001-7773-3809
Jeonghwan Hwang	http://orcid.org/0000-0002-1079-6634	Yongheum Jo	http://orcid.org/0000-0003-2425-389X
Jae-Kwang Lee	http://orcid.org/0000-0003-3903-0904	Jang-Soon Kwon	http://orcid.org/0000-0002-1826-6443

This is an Open-Access article distributed under the terms of the Creative Commons Attribution Non-Commercial License (http://creativecommons.org/licenses/by-nc/3.0) which permits unrestricted non-commercial use, distribution, and reproduction in any medium, provided the original work is properly cited

1. Introduction

Responsible management of spent nuclear fuel (SNF) has emerged as a significant issue in many countries utilizing nuclear power, and the concept of deep geological disposal (DGD) has been developed as the most practicable option for directly disposing of SNF without reprocessing [1]. Bentonite-based engineered barriers within a DGD system play key hydrogeochemical roles, particularly in preventing groundwater inflow to waste canisters and impeding migration of released radionuclides into the biosphere by providing abundant chemisorption sites [1-3]. The sorption properties of radionuclides onto mineral adsorbents have been widely interpreted and quantified using the concept of sorption-desorption partition (or distribution) coefficient (Kd). However, given that the Kd concept does not incorporate any specific reaction mechanisms, there is a clear limitation that an empirical Kd value depends on the experimental conditions under which it was evaluated. Accordingly, significant scientific efforts have been directed toward establishing a robust geochemical foundation for parameterizing the sorption phenomena more reliably, and thermodynamic sorption modeling (TSM) [4-6], which is chemically rooted in the law of mass action, was introduced with the aim of improving predictability in assessing the radionuclide retention in a DGD system across a wide range of geochemical conditions. Bentonite is naturally formed through the weathering of volcanic ash, and its characteristic swelling and chemisorption properties are predominated by montmorillonite, a planar 2:1 phyllosilicate that comprises the major portion (> 70wt%) of the clay's mineral content. Due to the heterogeneity of natural systems, montmorillonites from different origins have disparate mineral chemistry (e.g., degree of isomorphic substitution, interlayer cation composition, etc.), resulting in somewhat distinct thermal, hydrodynamic, mechanical, and chemical properties depending on their sources. Further, montmorillonites are generally categorized by their principal interlayer cations, and the most common forms discovered in nature are Na- and Ca-type montmorillonites. Thus far, Na-montmorillonite dominant bentonites (e.g., MX-80, Kunigel V1, etc.) have been thoroughly examined and selected as reference buffer materials for deep geological repositories (DGR) in numerous countries. However, recent experimental and theoretical studies have suggested that Ca-montmorillonite can display comparable or even more superior swelling capacity than Na-montmorillonite at high dry density (> 1.5 $g \cdot cm^{-3}$) [7-9], and most commercial Ca-bentonites indeed satisfy the mechanical criteria required as engineered barrier system (EBS) when formed into compressed blocks with a dry density greater than 1.6 $g \cdot cm^{-3}$ [10]. Yet, compared to Na-montmorillonite, there remains a scarcity of reported thermodynamic sorption data of important radionuclides onto Ca-montmorillonite from a perspective of high-level radioactive waste (HLW) disposal; ion-exchange behaviors of radionuclides onto montmorillonite definitely depend on the type of interlayer cations, and it has been reported that stability constants of relevant surface complexes formed at edge functionalities of montmorillonite vary noticeably between Na- and Ca-montmorillonites as well [11-14].

Korea Atomic Energy Research Institute (KAERI) adopted a new reference research Ca-bentonite in 2021, named Bentonil-WRK [15-18], as domestic KJ-I/-II Ca-bentonites are gradually being depleted in Korea. We aimed to develop a thermodynamic sorption database of radionuclides onto Ca-type Bentonil-WRK montmorillonite; as part of a national R&D program on SNF storage and disposal launched in 2021 [19], there has been a concerted effort to construct a comprehensive sorption database for various clay and crystalline rock minerals, which is aimed to be utilized as an essential input dataset in the operation of a process-based total system performance assessment framework, Apro [20]. In a previous study [17], we conducted experimental work on purifying Ca-montmorillonite from Bentonil-WRK bentonite, as well as investigating its acid-base properties and sorption interactions with Cs(I) and Sr(II), and it was confirmed that the experimental results can be satisfactorily modeled by simplifying the complicated reactive sorption

Table 1. Physico-chemical properties of purified Bentonil-WRK Ca-montmorillonite [17]

Parameters	Values
Cation exchange capacity	94.2 meq/100 g*
N_2 BET specific surface area	74.4 $m^2 \cdot g^{-1}$
Site density of edge aluminol group (≡AlOH)	$(4.94 \pm 0.12) \times 10^{-5}$ $mol \cdot g^{-1}$
Site density of edge silanol group (≡SiOH)	$(7.42 \pm 0.87) \times 10^{-5}$ $mol \cdot g^{-1}$
Surface reactions	**log K**
$X_2Ca + 2H^+ \rightleftharpoons 2XH + Ca^{2+}$	3.38 ± 0.06
$\equiv AlOH + H^+ \rightleftharpoons \equiv AlOH_2^+$	8.35 ± 0.24
$\equiv AlOH \rightleftharpoons \equiv AlO^- + H^+$	−9.59 ± 0.28
$\equiv SiOH \rightleftharpoons \equiv SiO^- + H^+$	−7.65 ± 0.09

* Adopted as a density of interlayer sorption site (X) of the montmorillonite

sites of montmorillonite into three types: interlayer sites with permanent negative charges, aluminol-like amphoteric edge sites, and silanol-like monoprotic edge sites. Se is another element of particular interest in the safety assessment of a DGR for HLW, owing to its long half-life of ^{79}Se radioisotope (3.27×10^5 years) and relatively high mobility in geological environments. Aqueous Se species undergo a range of redox reactions depending on Eh and pH of a solution, existing in oxidation states of Se(-II), Se(0), Se(IV), and Se(VI). Notably, Se(-II) and Se(0) form stable precipitates with significantly low solubilities under groundwater conditions [21, 22], while Se(VI) generally displays negligible sorption onto mineral phases [23, 24]. Se(IV) species, which display much stronger chemisorption affinities than Se(VI) species, are commonly formed in ambient aqueous solutions and can be released into EBS of a DGR under various scenarios of early waste canister failure, where oxidizing conditions persist. Further, investigating sorption mechanisms of Se(IV) onto mineral adsorbents is also essential for comprehending Se redox kinetics in geological media [25, 26], and these geochemical features render Se(IV) as the most interesting oxidation state of Se for elucidating its sorption thermodynamics onto natural mineral adsorbents. In this framework, continuing the previous study on sorption interactions between Bentonil-WRK montmorillonite and highly soluble fission products, this work presents examination and modeling of chemisorption behaviors of Se onto purified Ca-type Bentonil-WRK montmorillonite under ambient conditions (pH 4–9, pe 7–9, I = 0.01 M $CaCl_2$, and T = 25°C). The resulting experimental Kd and thermodynamic modeling data extend the material-specific sorption database of Bentonil-WRK and are fundamental for evaluating its chemical performance as a potential Ca-type buffer material of DGD system for HLW.

2. Experimental

2.1 Chemical Reagents and Clay Adsorbent

In this study, all experiments were performed under ambient conditions at 25 ± 1°C. Aqueous solution samples were prepared with deionized water, having a resistivity of 18.2 MΩ·cm at 25°C (Merck Millipore, Milli-Q Direct). The Se(IV) stock solution was prepared by dissolving precisely weighed H_2SeO_3 (Sigma-Aldrich, 99.999%) in deionized water, resulting in a total concentration of Se(IV) to be 0.01 M. The ionic strength and pH of experimental analytes were accurately adjusted using concentrated HCl (Sigma-Aldrich, 99.999%), $Ca(OH)_2$ (Sigma-Aldrich, 99.995%),

and $CaCl_2$ (Sigma-Aldrich, ≥ 99%) solutions. The homoionic Ca-montmorillonite, with a 95wt% purity, was separated from Bentonil-WRK bentonite (Clariant Korea) by performing the clay treatment processes as detailed in the previous work [17], and Table 1 summarizes the geochemical characterization of purified montmorillonite. The pH and pe of aqueous analytes were assessed using a combination pH electrode (Orion, 8107BN), an ORP (oxidation-reduction potential) electrode (Orion, 9179BN), and a meter (Orion, A326). The electrodes were freshly calibrated with standard pH and ORP buffer solutions (Orion), and the actual proton concentrations ($-\log [H^+] = pH_c$) were further corrected from the measured pH values based on an empirical approach detailed elsewhere [27-29], if necessary.

2.2 Batch Sorption Experiment

A total of 26 batch samples were prepared with a S/L ratio of 5 $g \cdot L^{-1}$ and two initial Se concentrations (=$[Se]_T$) of 0.05 and 0.11 mM to evaluate the kinetics and pH/pe-dependent sorption of Se onto the purified Ca-type Bentonil-WRK montmorillonite. Unfortunately, the use of radioactive Se isotopes (e.g., ^{75}Se and ^{79}Se), which offers advantages in a detection limit and accuracy for quantifying dissolved Se, was not available this study, and such sub-millimolar levels of $[Se]_T$ were taken into account by considering the weak sorption characteristics of Se onto clay minerals and the precision of inductively coupled plasma-mass spectrometry (ICP-MS) utilized for Se analysis. In detail, accurately weighed Bentonil-WRK Ca-montmorillonites were reacted with $CaCl_2$ solutions for 3 days where pH_c adjustments of the supernatants were made using HCl and $Ca(OH)_2$ solutions as required. Following the pretreatment of clay, defined amounts of Se(IV) stock solutions were added to the batch samples, and the suspensions were allowed to additionally equilibrate for 3 days in a bench-top incubated shaker (Lab Companion, IST-4075R). The reaction time was determined by considering the observed Se sorption kinetics evaluated at pH 5 (see Fig. 1), the

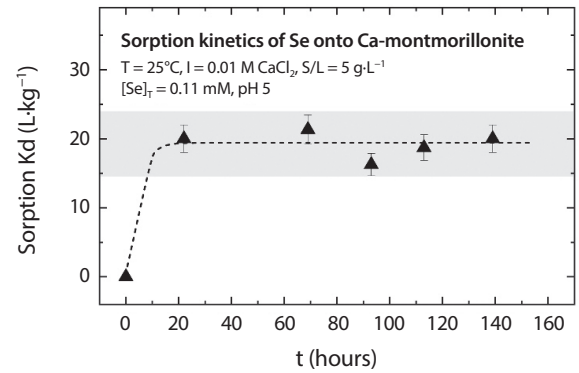

Fig. 1. Sorption kinetics of Se onto Ca-type Bentonil-WRK montmorillonite under the ambient conditions.

condition where Se sorption onto montmorillonite generally occurs most effectively. Subsequently, supernatant samples were separated from each mixture through centrifugation at 4,696 g for 10 minutes (Thermo Scientific, Sorvall X1 Pro), and final pH_c and pe of the solution phases were recorded. Aliquots of the supernatants were taken to determine dissolved concentrations of remaining Se and Al by ICP-MS (Perkin Elmer, NexION 350X); Al concentrations in all samples were below the detection limit (5 ppb), signifying that the centrifugal separation was successful. In addition to the 26 batch samples prepared to assess the sorption kinetics and thermodynamics of Se, an additional sample was made with a S/L ratio of 1 $g \cdot L^{-1}$ and relatively high $[Se]_T$ of 5 mM at pH_c 4.5. After the sorption reaction, all the Se-sorbed montmorillonite analytes were lyophilized, and their layered structure and morphology were analyzed by means of X-ray diffraction (XRD) and transmission electron microscope (TEM). Powder XRD spectra of the randomly oriented analytes were recorded on the diffractometer (Rigaku, SmartLab SE) with a Cu Kα source at 40 kV and 50 mA, where the measurement step size and acquisition time were 0.01° and 3 s per step, respectively. For TEM measurement, the lyophilized clay samples were ultrasonically dispersed in a pure ethanol medium (Sigma-Aldrich, 200 proof), and 5 μL of the dispersion solution was placed on a copper grid and dried. The morphology of Se-sorbed montmorillonite analytes was finally measured using a field-emission TEM

equipment (Hitachi HF5000) at an acceleration voltage of 200 kV with a cold field-emission electron gun.

2.3 Geochemical Speciation and Thermodynamic Sorption Modeling

The geochemical modeling programs PHREEQC [30] and PhreePlot [31] were utilized to compute the species distribution of Se in the present aquatic system and illustrate a corresponding Pourbaix diagram. Thermodynamic data required in the speciation were taken from Thermo-Chimie DB v12a [32] where activities of aqueous species were adjusted using the Davies equation [33]. The parameter estimation code PEST [34] was employed in conjunction with the PHREEQC to scrutinize the batch sorption data and refine the formation constants of associated surface Se complexes; within the geochemical calculations, thermodynamic activities of surface species involved were considered equivalent to their respective mole fractions for each sorption site. The diffuse double layer model (DDLM) [35] was adopted to correct the electrostatic effect in the assessment of chemisorption interactions at the solid-solution interface.

3. Results and Discussion

3.1 Aqueous Species Distribution of Se Under the Experimental Conditions

Fig. 2 displays the measured pH_c and pe of supernatants separated from the batch samples after sorption equilibrium of Se onto the Ca-montmorillonite was attained. The correlation between the pH_c and pe values obtained is evident, and it is expressed by a linear equation as shown in Equation (1). This implies that dissolved Se species or trace amounts of redox-active impurities (e.g., Fe, Mn, etc.) contained in the clay mineral may effectively function as redox

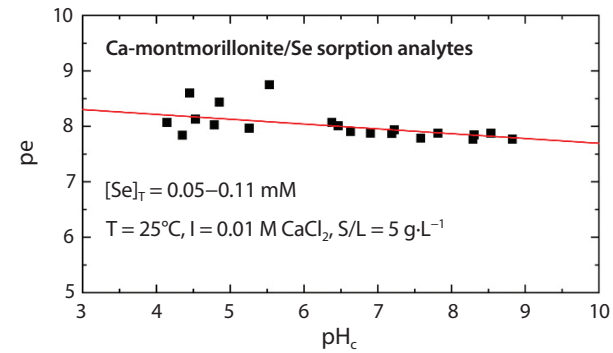

Fig. 2. A correlation between the measured pH_c and pe values of supernatants in the batch sorption analytes.

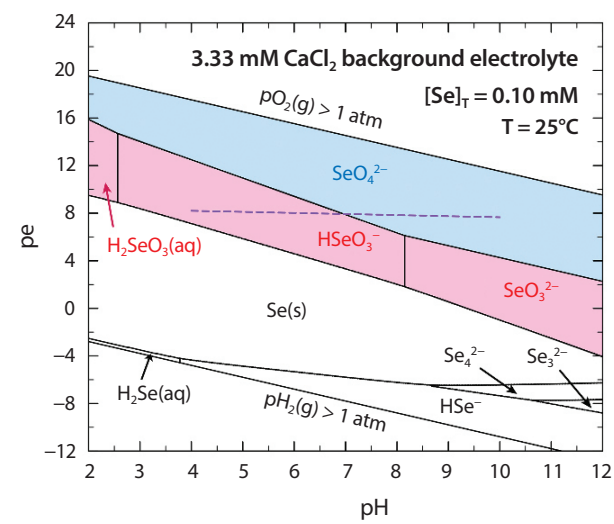

Fig. 3. Pourbaix diagram of Se where the violet dashed segment indicates the observed pH-pe correlation in the batch samples prepared in this study.

buffers in the present aquatic system.

$$pe = 16.9 \times Eh(V) = 8.56 - 0.09 \times pH_c \quad (\text{at } 25°C) \qquad (1)$$

pH and pe-dependent distribution of relevant aqueous Se species in a solution with 3.33 mM $CaCl_2$ background electrolyte was calculated, and Fig. 3 displays a resulting Pourbaix diagram ($[Se]_T$ = 0.1 mM and T = 25°C). It clearly shows that Se(IV) and Se(VI) are the two primary oxidation states of Se under the ambient conditions without precipitation, while the predominance of Se(0) and Se(-II) states generally increase as pe decreases across the entire

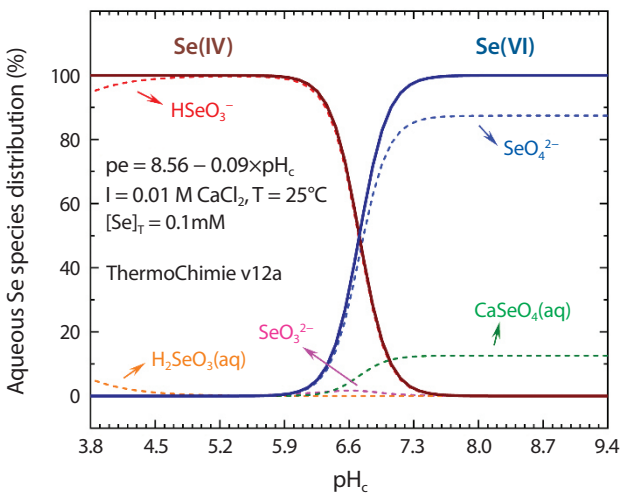

Fig. 4. pH_c-dependent distribution of aqueous Se species under the ambient conditions.

pH range. Additionally, Fig. 4 shows a more detailed pH_c-dependent distribution of aqueous Se species under the ambient conditions with the pe values being reflected according to Equation (1); at $pH_c < 6.7$, the majority of dissolved Se(IV) exist as $HSeO_3^-$ where minor H_2SeO_3(aq) and SeO_3^{2-} occupy less than 5% of $[Se]_T$, and the biselenite ion is progressively oxidized under alkaline conditions to form SeO_4^{2-} and $CaSeO_4$(aq) species.

3.2 Sorption Thermodynamics of Se(IV) Onto Ca-type Bentonil-WRK Montmorillonite

Table 2 provides the determined Kd values for Se sorption onto Bentonil-WRK Ca-montmorillonite by the batch experiment, except for a datum from the sorption kinetic measurement at t < 20 hours, and Fig. 5 displays the comparisons between experimental Kd data (open symbols) and TSM results (closed symbols). Since formation of relevant solid Se phases, such as SeO_2(s), $CaSeO_3 \cdot H_2O$(s), and $CaSeO_4 \cdot 2H_2O$(s), is generally excluded under the present Ca-H-Cl-CO_3-OH solution system, the slight but evident decrease in dissolved Se concentrations in the supernatants is attributed to the chemisorption of Se onto montmorillonite. The Kd values become negligible under alkaline conditions at $pH_c > 8$, where aqueous Se(VI) species are dominantly formed in the solution phase ($pe \approx 8.56 - 0.09 \times pH_c$), implying that only Se(IV) is the oxidation state responsible for Se sorption onto Bentonil-WRK montmorillonite under the experimental conditions considering the acid-base characteristics of aluminol groups in montmorillonite [17]. Dissimilar to most cationic species (e.g., Cs^+, Sr^{2+}, UO_2^{2+}, etc.), penetration of Se(IV) into the interlayer space of montmorillonite is typically ruled out at $pH_c > 4$ due to its negatively charged nature, and solely surface complexation of selenite species with the clay's edge functional groups is considered responsible for the adsorption behaviors. Indeed, XRD and TEM analyses of the Se(IV)-sorbed montmorillonite samples confirmed that their layered structure and morphology remained identical to that of unreacted Bentonil-WRK montmorillonite as shown in Fig. 6; XRD signals for the 001 diffraction of both analytes were observed at an identical 2θ position of 6.6° with FWHM of 1.3°, corresponding to a basal spacing (d_{001}) of 13.4 Å.

Regarding the possible chemisorption mechanisms of Se(IV) onto montmorillonite, binuclear-bidentate inner-sphere complexation [36] and outer-sphere complexation [26, 37] of selenite onto the edge aluminol site of mineral were individually proposed in the previous studies that employed X-ray absorption spectroscopy (XAS) to investigate Se(IV)-sorbed clay analytes; both inner- and outer-sphere Se(IV) complexations may indeed occur concurrently onto clay minerals, with the distribution of surface Se(IV) species governed by the experimental conditions. Moreover, another Se(IV) sorption study onto MX-80 bentonite [38] showed that, through parametric modeling of sorption data, a ternary surface Se(IV) species involving divalent background cations (Ca^{2+} and Mg^{2+}) can be formed. Complying with the simplified surface acid-base model of Bentonil-WRK montmorillonite (Table 1), chemical equations for the inner-sphere complexation, outer-sphere complexation, and ternary complexation of Se(IV) can be expressed as Equations (2), (3), and (4), respectively. In this study, two Se(IV) chemisorption reaction models, designated as model

Table 2. Experimental Kd values for Se sorption onto purified Bentonil-WRK Ca-montmorillonite evaluated in this study

Kd ($L \cdot kg^{-1}$)	pH_c	pe	$[Se]_T$	Kd ($L \cdot kg^{-1}$)	pH_c	pe	$[Se]_T$
9.2 ± 1.0	4.5	8.1	0.05 mM	17.9 ± 1.7	4.9	8.4	0.05 mM
20.7 ± 2.2	5.3	8.0	0.05 mM	4.2 ± 0.5	6.5	8.0	0.05 mM
4.1 ± 0.4	6.9	7.9	0.05 mM	4.1 ± 0.4	7.2	7.9	0.05 mM
4.0 ± 0.4	7.8	7.9	0.05 mM	−0.9 ± 0.1	8.3	7.8	0.05 mM
1.5 ± 0.1	8.5	7.9	0.05 mM	20.0 ± 2.1	4.9	8.5	0.11 mM
21.3 ± 2.2	5.1	8.3	0.11 mM	16.3 ± 1.6	5.0	8.2	0.11 mM
18.7 ± 2.0	4.8	8.2	0.11 mM	20.0 ± 2.1	4.9	8.1	0.11 mM
19.7 ± 2.0	4.1	8.1	0.11 mM	10.6 ± 1.1	4.4	7.8	0.11 mM
9.4 ± 1.0	4.5	8.6	0.11 mM	14.9 ± 1.6	4.8	8.0	0.11 mM
8.1 ± 0.8	5.5	8.8	0.11 mM	12.0 ± 1.2	6.4	8.1	0.11 mM
10.6 ± 1.2	6.6	7.9	0.11 mM	2.8 ± 0.3	7.2	7.9	0.11 mM
5.4 ± 0.5	7.6	7.8	0.11 mM	0.3 ± 0.1	8.3	7.9	0.11 mM
0.3 ± 0.1	8.9	7.7	0.11 mM		-		

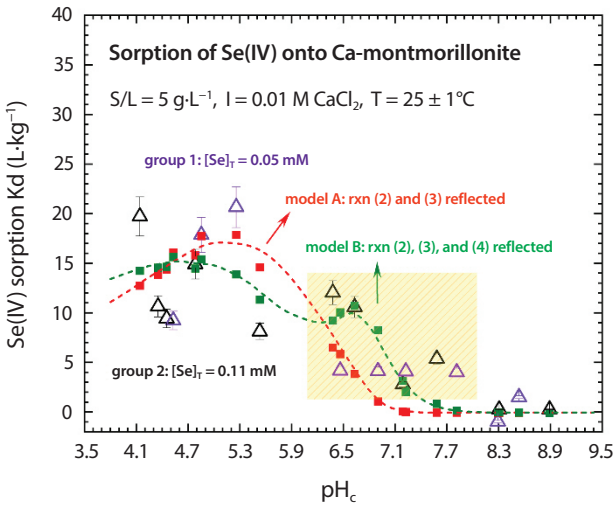

Fig. 5. Assessed Kd values for Se(IV) sorption onto purified Bentonil-WRK Ca-montmorillonite and their comparisons with the TSM results.

A and B, were then examined in the TSM of experimental data; model A reflects both the inner- and outer-sphere complexation mechanisms supported by spectroscopic evidence, while model B is a more comprehensive reaction model that incorporates the ternary complexation mechanism as well.

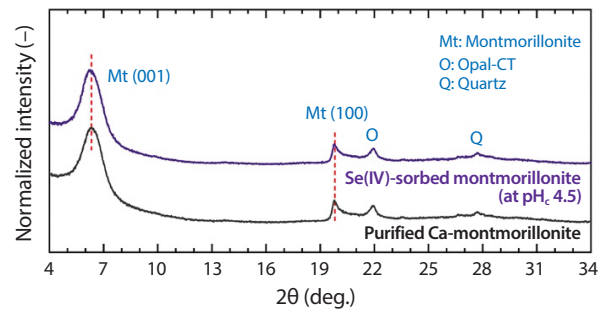

(a)

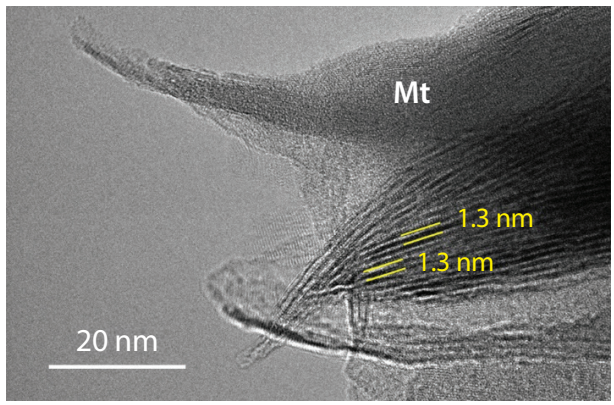

(b)

Fig. 6. Representative results of (a) XRD and (b) TEM analyses of the Se(IV)-sorbed montmorillonite prepared with a S/L ratio of 1 $g \cdot L^{-1}$ and $[Se]_T$ of 5 mM at pH_c 4.5.

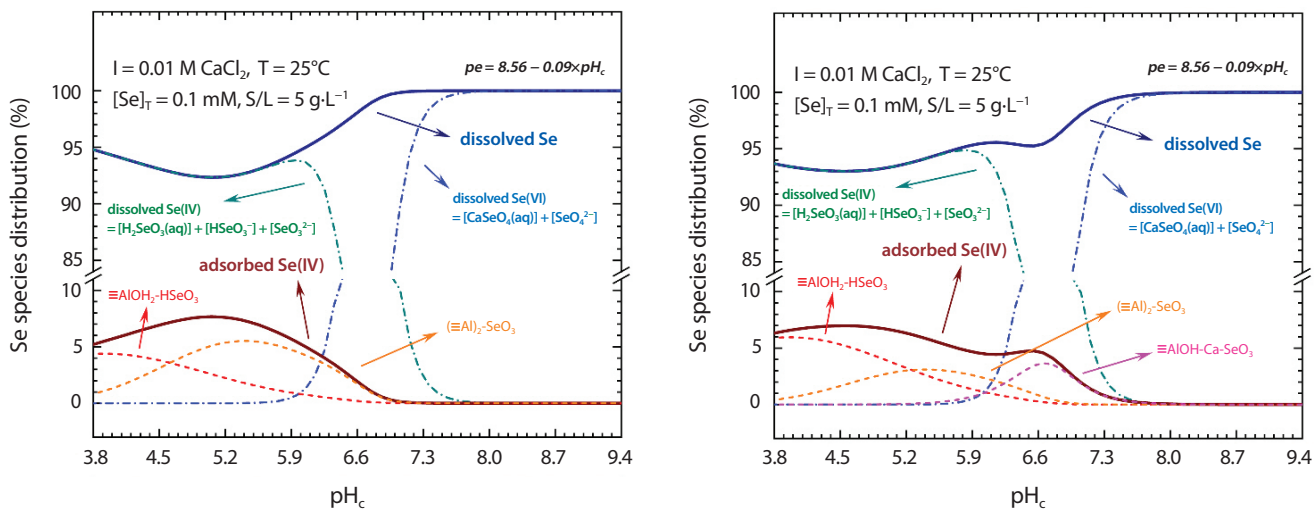

(a) Sorption model A

(b) Sorption model B

Fig. 7. pH_c-dependent species distribution of Se sorbed onto Bentonil-WRK Ca-montmorillonite at pe = 8.56 − 0.09×pH_c, I = 0.01 M $CaCl_2$, S/L = 5 g·L^{-1}, T = 25°C, and $[Se]_T$ = 0.1 mM based on chemisorption reaction (a) model A and (b) model B.

$$2{\equiv}AlOH + H_2SeO_3(aq) \rightleftharpoons ({\equiv}Al)_2SeO_3 + 2H_2O(l) \quad (2)$$

$${\equiv}AlOH_2^+ + HSeO_3^- \rightleftharpoons {\equiv}AlOH_3SeO_3 \quad (3)$$

$${\equiv}AlOH + Ca^{2+} + SeO_3^{2-} \rightleftharpoons {\equiv}AlOHCaSeO_3 \quad (4)$$

The red and green marks in Fig. 5 denote the re-calculated Se(IV) Kd values under the present aqueous conditions, obtained through TSM of the experimental data using the reaction models A and B, respectively. Both models acceptably simulate the pH_c-dependent chemisorption behaviors of Se(IV) under acidic conditions, while the TSM based on model B indicates slightly more effective Se(IV) adsorption onto Bentonil-WRK montmorillonite at pH_c 6–8, attributed to the formation of an additional $\equiv AlOHCaSeO_3$ surface complex; this renders it somewhat more suitable compared to the TSM based on model A. Nevertheless, it cannot be conclusively asserted that chemisorption model A should be excluded from the TSM, as spectroscopic evidence supporting the formation of ternary Se(IV) species is lacking. Hence, we present the TSM results based on both reaction models in this study, and Table 3 summarizes the determined equilibrium constants for each chemisorption reaction mechanism along with their uncertainties corresponding to a 95% confidence level. Fig. 7 displays the assessed distribution of surface Se(IV) species sorbed onto Bentonil-WRK Ca-montmorillonite under aqueous conditions of pH_c 4–9, pe = 8.56 − 0.09 × pH_c, I = 0.01 M $CaCl_2$, S/L = 5 g·L^{-1}, T = 25°C, and $[Se]_T$ = 0.1 mM using the resulting thermodynamic sorption data in this study. Both chemisorption reaction models similarly simulate the decreasing trend of Se(IV) Kd values as the pH_c of supernatant increases, with outer-sphere and inner-sphere complexes are identified as the major surface species in acidic and near-acidic conditions, respectively. According to model B, the ternary Se(IV) complexation is anticipated to occur only in a narrow neutral pH_c region. The calculated surface Se species distributions generally align with the previously reported pH-dependent sorption characteristics of Se(IV) onto bentonites or montmorillonites from different origins (e.g., MX-80, Kunigel V1, FEBEX, GMZ, etc.) [23, 38-47]. However, unfortunately, there are no available log K data directly comparable to those determined in this study, as the other relevant TSM studies [23, 38, 40-46] adopted

Table 3. Resulting equilibrium constants for the assumed surface reaction mechanisms of Se(IV) onto Bentonil-WRK Ca-montmorillonite

Chemisorption reaction model	Surface reaction	log K
Model A	$\equiv AlOH_2^+ + HSeO_3^- \rightleftharpoons \equiv AlOH_3SeO_3$	0.36 ± 0.33
	$2\equiv AlOH + H_2SeO_3(aq) \rightleftharpoons (\equiv Al)_2SeO_3 + 2H_2O(l)$	8.18 ± 0.32
Model B	$\equiv AlOH_2^+ + HSeO_3^- \rightleftharpoons \equiv AlOH_3SeO_3$	0.50 ± 0.21
	$2\equiv AlOH + H_2SeO_3(aq) \rightleftharpoons (\equiv Al)_2SeO_3 + 2H_2O(l)$	7.89 ± 0.51
	$\equiv AlOH + Ca^{2+} + SeO_3^{2-} \rightleftharpoons \equiv AlOHCaSeO_3$	7.69 ± 0.28

different surface reaction models (i.e., types of simplified functionalities considered, reaction stoichiometry, electrostatic correction approach, etc.) to interpret their experimental data.

4. Concluding Remark

Sorption behaviors of highly soluble radionuclides onto montmorillonite, a major mineral component of bentonite clay, should be thoroughly examined to accurately assess the transport of radionuclides in EBS of a DGR for HLW. The application of TSM enhances confidence and predictability in geochemical modeling of radionuclide retention by mineral adsorbents compared to the conventional Kd-based approach. In the present work, we investigated pH and pe-dependent Se sorption properties onto Ca-montmorillonite purified from Bentonil-WRK—a new reference research clay introduced by KAERI—under ambient conditions by conducting batch experiment and DDLM-based TSM following the simplified surface acid-base model for Bentonil-WRK described in the previous study [17]. This is part of a national R&D project [19] on construction of a robust sorption database for the Ca-bentonite, which is being developed in conjunction with a process-based total system performance assessment framework, APro [20]. The established material-specific surface reaction models and associated equilibrium constants successfully reproduced the observed Se(IV) sorption properties over the studied aqueous conditions, where outer-sphere complexation, inner-sphere complexation, and formation of Ca-involved ternary complex of Se(IV) onto edge aluminol groups of montmorillonite were considered; outer-sphere and inner-sphere Se(IV) complexes are identified as major surface species formed under acidic (pH ≈ 4) and near-acidic (pH ≈ 6) conditions, respectively, and the ternary Se(IV) complexation with Ca^{2+} background cation can occur at neutral pHs. Further sorption studies on Ca-type Bentonil-WRK montmorillonite should focus on expanding the spectrum of target adsorbates (e.g., actinides, iodine, simple organics, etc.) under a broader range of aquatic conditions relevant to the DGD environment, including high temperature, hyperalkaline, and saline conditions, as quantitative sorption data produced under such geochemical conditions is certainly lacking compared to that evaluated under ambient systems.

Conflict of Interest

The authors declare that they have no known competing financial interests or personal relationships that could have appeared to influence the work reported in this paper.

Acknowledgements

This study was supported by the Institute for Korea Spent Nuclear Fuel (iKSNF) and National Research Foundation

of Korea (NRF) grant funded by the Korean Ministry of Science and ICT (Grant code: 2021M2E1A1085202).

REFERENCES

[1] M.J. Apted and J. Ahn, Geological Repository Systems for Safe Disposal of Spent Nuclear Fuels and Radioactive Waste, 2nd ed., Woodhead Publishing, Duxford, UK (2017).

[2] OECD Nuclear Energy Agency. International Features, Events and Processes (IFEP) List for the Deep Geological Disposal of Radioactive Waste Version 3.0, OECD Nuclear Energy Agency Report, NEA/RWM/R(2019)1 (2019).

[3] K. Son, K. Choi, J. Yang, H. Jeong, H. Kim, K. Chang, and G. Heo, "A Review of the Features, Events, and Processes and Scenario Development for Korean Risk Assessment of a Deep Geological Repository for High-Level Radioactive Waste", Nucl. Eng. Technol., 55(11), 4083-4095 (2023).

[4] V. Brendler, A. Vahle, T. Arnold, G. Bernhard, and T. Fanghänel, "RES3T-Rossendorf Expert System for Surface and Sorption Thermodynamics", J. Contam. Hydrol., 61(1-4), 281-291 (2003).

[5] M. Ochs, J.A. Davis, M. Olin, T.E. Payne, C.J. Tweed, M.M. Askarieh, and S. Altmann, "Use of Thermodynamic Sorption Models to Derive Radionuclide Kd Values for Performance Assessment: Selected Results and Recommendations of the NEA Sorption Project", Radiochim. Acta, 94(9-11), 779-785 (2006).

[6] T.E. Payne, V. Brendler, M. Ochs, B. Baeyens, P.L. Brown, J.A. Davis, C. Ekberg, D.A. Kulik, J. Lutzenkirchen, T. Missana, Y. Tachi, L.R. Van Loon, and S. Altmann, "Guidelines for Thermodynamic Sorption Modelling in the Context of Radioactive Waste Disposal", Environ. Model. Softw., 42, 143-156 (2013).

[7] O. Karnland, S. Olsson, and U. Nilsson. Mineralogy and Sealing Properties of Various Bentonites and Smectite-Rich Clay Materials, Swedish Nuclear Fuel and Waste Management Company Technical Report, TR-06-30 (2006).

[8] L. Sun, J.T. Hirvi, T. Schatz, S. Kasa, and T.A. Pakkanen, "Estimation of Montmorillonite Swelling Pressure: A Molecular Dynamics Approach", J. Phys. Chem. C, 119(34), 19863-19868 (2015).

[9] B. Akinwunmi, J.T. Hirvi, S. Kasa, and T.A. Pakkanen, "Swelling Pressure of Na- and Ca-Montmorillonites in Saline Environments: A Molecular Dynamics Study", Chem. Phys., 528, 110511 (2020).

[10] M. Kim, J. Lee, S. Yoon, S. Choi, M. Kong, and J.S. Kim. Comparison and Analysis of Physical Properties Database for Buffer Material Candidates, Korea Atomic Energy Research Institute Technical Report, KAERI/TR-9795/2023 (2023).

[11] M.H. Bradbury and B. Baeyens, "Modelling the Sorption of Zn and Ni on Ca-montmorillonite", Geochim. Cosmochim. Acta, 63(3-4), 325-336 (1999).

[12] M.H. Bradbury and B. Baeyens, "Sorption of Eu on Na- and Ca-montmorillonites: Experimental Investigations and Modelling With Cation Exchange and Surface Complexation", Geochim. Cosmochim. Acta, 66(13), 2325-2334 (2002).

[13] M.H. Bradbury and B. Baeyens, "Modelling Sorption Data for the Actinides Am(III), Np(V) and Pa(V) on Montmorillonite", Radiochim. Acta, 94(9-11), 619-625 (2006).

[14] M. Ghayaza, L. Le Forestier, F. Muller, C. Tournassat, and J.M. Beny, "Pb(II) and Zn(II) Adsorption Onto Na- and Ca-montmorillonites in Acetic Acid/Acetate Medium: Experimental Approach and Geochemical Modeling", J. Colloid Interface Sci., 361(1), 238-246 (2011).

[15] G.J. Lee, S. Yoon, and B.J. Kim, "Prediction Model for Saturated Hydraulic Conductivity of Bentonite Buffer Materials for an Engineered-Barrier System in a High-Level Radioactive Waste Repository", J. Nucl. Fuel Cycle Waste Technol., 21(2), 225-234 (2023).

[16] J.Y. Goo, B.J. Kim, J.S. Kwon, and H.Y. Jo, "Bentonite Alteration and Retention of Cesium and Iodide Ions by Ca-bentonite in Alkaline and Saline Solutions", Appl. Clay Sci., 245, 107141 (2023).

[17] S. Choi, B.J. Kim, S. Seo, J.K. Lee, and J.S. Kwon, "Characterization of the Purified Ca-type Bentonil-WRK Montmorillonite and Its Sorption Thermodynamics With Cs(I) and Sr(II)", J. Nucl. Fuel Cycle Waste Technol., 21(4), 427-438 (2023).

[18] S. Yoon, G.J. Lee, D.H. Lee, M.S. Kim, J.T. Kim, and J.S. Kim, "Evaluation of Thermal Properties for the Bentonil-WRK Bentonite", J. Nucl. Fuel Cycle Waste Technol., 22(1), 9-16 (2024).

[19] K. Kim, "iKSNF, the Control Tower for the R&D Program of SNF Storage and Disposal", J. Nucl. Fuel Cycle Waste Technol., 20(2), 255-258 (2022).

[20] J.W. Kim, H. Jang, D.H. Lee, H.H. Cho, J. Lee, M. Kim, and H. Ju, "A Modularized Numerical Framework for the Process-based Total System Performance Assessment of Geological Disposal Systems", Nucl. Eng. Technol., 54(8), 2828-2839 (2022).

[21] H.R. Cho, H.K. Kim, W. Cha, H. Ju, J. Kim, K. Kim, and W. Um. Analysis of the Solubilities of Radioactive Materials in Oxidative Groundwater Conditions – Geochemical Modeling, Korea Atomic Energy Research Institute Technical Report, KAERI/TR-9156/2022 (2022).

[22] H.K. Kim, W. Cha, T.H. Kim, and H.R. Cho. Thermodynamic Evaluation of Solubility and Aqueous Chemical Reactions of Radionuclides Under KURT Groundwater Conditions: 21 Radionuclides, Korea Atomic Energy Research Institute Technical Report, KAERI/TR-9797/2023 (2023).

[23] S. Goldberg, "Modeling Selenite Adsorption Envelopes on Oxides, Clay Minerals, and Soils Using the Triple Layer Model", Soil Sci. Soc. Am. J., 77(1), 64-71 (2013).

[24] S. Goldberg, "Modeling Selenate Adsorption Behavior on Oxides, Clay Minerals, and Soils Using the Triple Layer Model", Soil Sci., 179(12), 568-576 (2014).

[25] R.H. Neal and G. Sposito, "Selenium Mobility in Irrigated Soil Columns as Affected by Organic Carbon Amendment", J. Environ. Qual., 20(4), 808-814 (1991).

[26] L. Charlet, A.C. Scheinost, C. Tournassat, J.M. Greneche, A. Géhin, A. Fernández-Martínez, S. Coudert, D. Tisserand, and J. Brendle, "Electron Transfer at the Mineral/Water Interface: Selenium Reduction by Ferrous Iron Sorbed on Clay", Geochim. Cosmochim. Acta, 71(23), 5731-5749 (2007).

[27] Th. Fanghänel, V. Neck, and J.I. Kim, "The Ion Product of H_2O, Dissociation Constants of H_2CO_3 and Pitzer Parameters in the System $Na^+/H^+/OH^-/HCO_3^-/CO_3^{2-}/ClO_4^-/H_2O$ at 25°C", J. Solution Chem., 25(4), 327-343 (1996).

[28] M. Altmaier, V. Metz, V. Neck, R. Müller, and Th. Fanghänel, "Solid-Liquid Equilibria of $Mg(OH)_2$(cr) and $Mg_2(OH)_3Cl{\cdot}4H_2O$(cr) in the System Mg-Na-H-OH-Cl-H_2O at 25°C", Geochim. Cosmochim. Acta, 67(19), 3595-3601 (2003).

[29] S. Choi and J.I. Yun, "Spectrophotometric Study of the Uranyl Monobenzoate Complex at Moderate Ionic Strength", Polyhedron, 161, 120-125 (2019).

[30] D.L. Parkhurst and C.A.J. Appelo, Description of Input and Examples for PHREEQC Version 3: A Computer Program for Speciation, Batch-Reaction, One-Dimensional Transport, and Inverse Geochemical Calculations, U.S. Geological Survey, Reston, VA (2013).

[31] D.G. Kinniburgh and D.M. Cooper, PhreePlot: Creating Graphical Output With PHREEQC (2011).

[32] E. Giffaut, M. Grivé, Ph. Blanc, Ph. Vieillard, E. Colàs, H. Gailhanou, S. Gaboreau, N. Marty, B. Madé, and L. Duro, "Andra Thermodynamic Database for Performance Assessment: ThermoChimie", Appl. Geochem., 49, 225-236 (2014).

[33] I. Grenthe, F. Mompean, K. Spahiu, and H. Wanner, TDB-2 Guidelines for the Extrapolation to Zero Ionic Strength, OECD Nuclear Energy Agency, Issy-les-Moulineaux, France (2013).

[34] J. Doherty, Calibration and Uncertainty Analysis for Complex Environmental Models, Watermark Numerical Computing, Brisbane, Australia (2015).

[35] J. Lützenkirchen, R. Marsac, D.A. Kulik, T.E. Payne, Z. Xue, S. Orsetti, and S.B. Haderlein, "Treatment of Multi-Dentate Surface Complexes and Diffuse Layer Implementation in Various Speciation Codes", Appl. Geochem., 55, 128-137 (2015).

[36] D. Peak, U.K. Saha, and P.M. Huang, "Selenite Adsorption Mechanisms on Pure and Coated Montmorillonite: An EXAFS and XANES Spectroscopic Study", Soil Sci. Soc. Am. J., 70(1), 192-203 (2006).

[37] W. Xu, H.B. Qin, J.M. Zhu, T.M. Johnson, D. Tan, C. Liu, and Y. Takahashi, "Selenium Isotope Fractionation During Adsorption Onto Montmorillonite and Kaolinite", Appl. Clay Sci., 211, 106189 (2021).

[38] G. Montavon, Z. Guo, J. Lützenkirchen, E. Alhajji, M.A.M. Kedziorek, A.C.M. Bourg, and B. Grambow, "Interaction of Selenite With MX-80 Bentonite: Effect of Minor Phases, pH, Selenite Loading, Solution Composition and Compaction", Colloids Surf. A: Physicochem. Eng. Asp., 332(2-3), 71-77 (2009).

[39] B. Bar-Yosef and D. Meek, "Selenium Sorption by Kaolinite and Montmorillonite", Soil Sci., 144(1), 11-19 (1987).

[40] S. Goldberg and R.A. Glaubig, "Anion Sorption on a Calcareous, Montmorillonitic Soil-Selenium", Soil. Sci. Soc. Am. J., 52(4), 954-958 (1988).

[41] K.A. Boult, M.M. Cowper, T.G. Heath, H. Sato, T. Shibutani, and M. Yui, "Towards an Understanding of the Sorption of U(VI) and Se(IV) on Sodium Bentonite", J. Contam. Hydrol., 35(1-3), 141-150 (1998).

[42] P. Wang, A. Anderko, and D.R. Turner, "Thermodynamic Modeling of the Adsorption of Radionuclides on Selected Minerals. II: Anions", Ind. Eng. Chem. Res., 40(20), 4444-4455 (2001).

[43] T. Missana, U. Alonso, and M. García-Gutiérrez, "Experimental Study and Modelling of Selenite Sorption Onto Illite and Smectite Clays", J. Colloid Interface Sci., 334(2), 132-138 (2009).

[44] K. Shi, Y. Ye, N. Guo, Z. Guo, and W. Wu, "Evaluation of Se(IV) Removal From Aqueous Solution by GMZ Na-bentonite: Batch Experiment and Modeling Studies", J. Radioanal. Nucl. Chem., 299, 583-589 (2014).

[45] N. Mayordomo, U. Alonso, and T. Missana, "Analysis of the Improvement of Selenite Retention in Smectite by Adding Alumina Nanoparticles", Sci. Total Environ., 572, 1025-1032 (2016).

[46] J.P. Morel, N. Marmier, C. Hurel, and N. Morel-Desrosiers, "Thermodynamics of Selenium Sorption on Alumina and Montmorillonite", Cogent Chem., 1(1), 1070943 (2015).

[47] Y. Li, J. He, W. Zhou, Y. Shi, J. Wang, D. Xian, and C. Liu, "Influence of Colloids and Colloids' Coagulation on Selenite Sorption", Colloids Surf. A: Physicochem. Eng. Asp., 618, 126462 (2021).